Chemistry Europe
European Chemical Societies Publishing

WILEY VCH

Excellence in Chemistry Research

Announcing our new flagship journal

- Gold Open Access
- Publishing charges waived
- Preprints welcome
- Edited by active scientists

Meet the Editors of *ChemistryEurope*

Luisa De Cola
Università degli Studi di Milano Statale, Italy

Ive Hermans
University of Wisconsin-Madison, USA

Ken Tanaka
Tokyo Institute of Technology, Japan

Chemistry–A European Journal
Research Article
doi.org/10.1002/chem.202301061
Chemistry Europe
European Chemical Societies Publishing
www.chemeurj.org

Sugar-Bridged Fullerene Dumbbells and Their Interaction with the [10]Cycloparaphenylene Nanoring

Jovana Jakšić,[a] Iris Solymosi,[b] Andreas Hirsch,[b] M. Eugenia Pérez-Ojeda,*[b] Aleksandra Mitrović,*[a] and Veselin Maslak*[a]

Abstract: The synthesis and characterization of four dumbbell-shaped fullerene molecules connected by isosorbide and isomannide moieties is presented. Additionally, their electrochemical behavior and their ability to form complexes with [10]cycloparaphenylene ([10]CPP) were investigated. The cyclic voltammetry (CV) results of the fullerene dumbbells demonstrate a high electron affinity, indicating their strong interaction with electron-donating counterparts such as carbon nanorings, which possess complementary charge and shape properties. To study the thermodynamic and kinetic parameters of complexation, isothermal titration calorimetry (ITC) was employed. NMR titration experiments provided further insights into the binding stoichiometries. Two distinct approaches were utilized to create bridged structures: one based on cyclopropane and the other based on furan. Regardless of the type of linker used, all derivatives formed conventional 2:1 complexes denoted as [10]CPP$_2$⊃C$_{60derivative}$. However, the methano-dumbbell molecules exhibited distinct binding behavior, resulting in the formation of mono- and bis-pseudorotaxanes, as well as oligomers (polymers). The formation of linear polymers holds significant potential for applications in solar energy conversion processes.

Introduction

Fullerene dumbbell-shaped molecules structured as C_{60}-linkers-C_{60} are an important class of organic compounds, whose properties can be tailored. The linkers not only determine the geometry and accessibility of the fullerene but also serve as either electron donors or acceptors. Moreover, due to their spatial confinement near the C_{60} surface, these molecular arrangements present a promising avenue for designing innovative molecular electronic devices. It is crucial for the potential development of optoelectronic devices that these dumbbell molecules exhibit equal or superior electron-accepting capabilities compared to pristine C_{60}.[1] In the case of dumbbell-shaped C_{60}, the cage is predominantly functionalized by cyclopropanation,[2] 1,3-dipolar cycloaddition[3] or [4+2]-Diels–Alder reaction,[4] while the bridging of fullerene derivatives with versatile building blocks such as aliphatic chains,[5] perylene diimides (PDIs),[6] pyrromellitic diimides,[7] azobenzene,[1] biphenyl,[8] fluorene,[9] triazol,[10] BODIPY,[11] porphyrins,[12] transition metal complexes,[13] ferrocene,[14] TTF,[4b] among others, has been accomplished. Concurrently, C_{60} molecular dumbbells have also gained prominence in supramolecular chemistry, acting as guests in host–guest molecular recognition. Macrocyclic structures, exemplified by cycloparaphenylene [10]CPP with radial π-conjugation systems, have demonstrated suitability as hosts for C_{60} due to their optimal shape and size, allowing for multiple non-covalent interactions with the fullerene C_{60}.

The first example of complexes formed between [10]CPP and fullerene C_{60} proved that host–guest interactions were significantly enhanced by the convex-concave π-π interactions quantified in a solid-state structure.[15] These interactions facilitated a template approach in the synthesis of the initial [10]CPP-fullerene [2]rotaxanes.[16] It was discovered that the interlocked [10]CPP, when bound to the C_{60} in the axes, strongly affected the process of charge recombination by acting as an relay of positive charge.[17] Recently, Pérez-Ojeda's group published a comprehensive study on two dumbbell-like [60]fullerene systems, P1$(C_{60})_2$ and P2$(C_{60})_2$, and their interactions with ([10]CPP). The study demonstrated that the presence of a single (P1) or double (P2) perylene bisimide bridge between the fullerene moieties did not significantly affect the formation of complexes with [10]CPP. The complex formation was thoroughly investigated using spectroscopic and calorimetric techniques and compared to the reference system [10]CPP⊃C_{60}. Global analysis of the ITC titration data confirmed the formation of 2:1 complexes, with a single [10]CPP molecule binding each fullerene in an enthalpically driven complexation process.[18]

In this article, we report the synthesis of C_{60} fullerene dumbbell-like molecules bridged by a sugar and the formation of bis-pseudorotaxanes with [10]CPP. The sugar unit 1,4:3,6-dianhydrohexitols was chosen for having two nearly planar *cis*-

[a] J. Jakšić, Dr. A. Mitrović, Dr. V. Maslak
University of Belgrade
Faculty of Chemistry
Studentski trg 12–16, 11158 Belgrade (Serbia)
E-mail: afemic@chem.bg.c.rs
vmaslak@chem.bg.c.rs
[b] I. Solymosi, Prof. Dr. A. Hirsch, Dr. M. E. Pérez-Ojeda
Department of Chemistry and Pharmacy
Friedrich-Alexander-University Erlangen-Nuremberg
Nikolaus-Fiebiger-Str. 10, 91058 Erlangen (Germany)
E-mail: eugenia.perez-ojeda@fau.de

Supporting information for this article is available on the WWW under https://doi.org/10.1002/chem.202301061

fused five-membered rings in the form of a "V" with the hydroxyl groups located at the C_2- and C_5-positions either inside or outside the V-shaped wedge, which could affect both the position of the C_{60} spheres and the solubility of the dumbbells. The stereochemistry of the hydroxyl groups in cyclitols plays an important role in determining their properties. For example, cyclitols with the hydroxyl groups located inside the V-shaped wedge tend to have a more compact and rigid structure. In contrast, cyclitols with the hydroxyl groups located outside the V-shaped wedge tend to have a more open and flexible structure, which can affect their physical and chemical properties, including solubility and reactivity. As a result, the synthesized fullerene dumbbells are expected to exhibit different properties depending on the location of the hydroxyl groups in the V-shaped wedge. We used isomannide with two *endo*-hydroxyl groups and isosorbide with one *endo* at C_5 and one *exo* group at C_2.[19]

Results and Discussion

The dumbbell-shaped fullerene-sugar hybrids (**10_{IS}**, **11_{IM}**, **12_{IS}**, **13_{IM}**, Scheme 1) were obtained via a multi-step synthetic pathway in which pristine fullerene C_{60} was covalently attached to the sugar by cyclopropanation or a [3 + 2] cycloaddition reaction according to Bingel-Hirsch protocol, which involves the preparation of the corresponding bis-β-keto ester-sugar derivatives. In Scheme 1A, the first step requires the preparation of the sugar derivates **6** and **8**. The hydrolysis of the β-keto ester prepared from Meldrum acid and hexanoyl chloride gave 3-oxooctanoic acid in 81% yield, which served as the starting material (see Supporting Information, Scheme S1).

The reactions were conducted in dichloromethane (DCM) for 24 h at room temperature, using 2 equivalents of **4** and commercial isosorbide and isomannide in the presence of *N*,*N*′-dicyclohexylcarbodiimide (DCC) and 4-dimethylaminopyridine (DMAP). Compounds **6** and **8** were obtained with 60% and 62% yields, respectively.

In a recent study, we presented an efficient synthesis of furan-fused fullerenes, where various derivatives were prepared by a simple reaction of medium-chain β-keto esters and C_{60} in the presence of diazabicyclo[5.4.0]undec-7-ene (DBU) using 2,2,6,6-tetramethylpiperidine-1-oxyl (TEMPO) in toluene for 45 min at room temperature.[20] To further advance our research, we prepared dumbbell-like furan-fused fullerenes **10_{IS}**, **11_{IM}** under the same reaction conditions used for the generation of monoadducts. By attaching two C_{60} units to bis-β-keto esters **6**, **8** through a double [3 + 2] cycloaddition reaction, we obtained yields of 17–18% (Scheme 1, B). This allowed us to incorporate a sugar unit as a bridge between the two C_{60} moieties.

The first step involved a double [3 + 2] cycloaddition of (3*R*,3a*S*,6*S*,6a*S*)-hexahydrofuro[3,2-b]furan-3,6-diyl bis(3-oxooctanoate) **6** was carried out with C_{60} fullerene containing 1.5 equivalents of **9**, 20 equivalents of DBU and the addition of 2 equivalents of TEMPO, the yield of **10_{IS}** was 17% (or 41% per C_{60} unit) (see Table S1, entry 3, Supporting Information). When the cycloaddition reaction of **6** was performed with 2 or 3 equivalents of **9**, the yield of **10_{IS}** increased to 19% and 24%, respectively (see Table S1, entries 4–5). A similar result was obtained when 3 equivalents of **9** were used in the presence of 40 equivalents of DBU and 4 equivalents of TEMPO (see Table S2, entry 6). In contrast, using 1 equivalent of **9** resulted in a lower yield of **10_{IS}** at only 7% (Table S2, entry 2, Supporting Information). Additionally, reducing the amount of C_{60} fullerene to 0.5 equivalents did not yield the desired product (see Table S2, entry 1, Supporting Information). These findings indicate that increasing the amount of C_{60} in the double [3 + 2] cycloaddition reaction with **6** gradually reduces the yield of **10_{IS}**, while increasing the amount of DBU and TEMPO has minimal impact. Alternatively, using the Bingel-Hirsch protocol we obtained the dumbbell-like methanofullerenes **12_{IS}**, **13_{IM}** by reacting C_{60} **9** with the bis-β-keto ester-sugar derivatives **6**, **8**, iodine, and DBU in toluene at room temperature for 45 min, yielding 14–15% (Scheme 1, C).

The dumbbell-shaped dihydrofuran-fused fullerenes **10_{IS}**, **11_{IM}** and dumbbell-shaped methanofullerenes **12_{IS}**, **13_{IM}** were synthesized for the first time. Their structures were confirmed by HRMS, ^{1}H NMR, ^{13}C NMR, FTIR and UV-Vis. These products exhibit significant solubility in common organic solvents such as toluene, DCM and chloroform, with solubilities ranging from approximately 2 to 5 mg mL^{-1}. The solubility of **11_{IM}**, determined using UV-Vis spectroscopy as a representative example, was found to be 2.8 mg mL^{-1} in toluene, which is on par with the solubility of C_{60} alone. This excellent solubility is particularly beneficial for the two C_{60} dumbbells. This solubility property of the dumbbell-like furan-fused fullerenes is crucial for their potential applications and their feasibility in materials chemistry.[21] (the procedure is described in the Supporting Information).

The electrochemical properties of C_{60} and dumbbell-like **10_{IS}**,**11_{IM}** and **12_{IS}**, **13_{IM}** were studied by cyclic voltammetry (CV) and linear sweep voltammetry (LSV) at room temperature using tetrabutylammonium hexafluorophosphate (nBu$_4$NPF$_6$) (0.1 M) as a supporting electrolyte in *o*-dichlorobenzene/dimethylformamide (*o*-DCB/DMF 100 : 1 *v*/*v*) as the solvent. The resulting CV and LSV data are listed in Table 1. The obtained products **10_{IS}**, **11_{IM}** and **12_{IS}**, **13_{IM}** showed four reversible reduction waves, corresponding to the successive reductions of the C_{60} cage (Figure S37–S41). Both types of dumbbells **10_{IS}**, **11_{IM}** and **12_{IS}**, **13_{IM}** exhibited a higher electron affinity than pristine C_{60}. The first reduction potentials E_{red} of the reaction products is similar

Table 1. Half-wave reduction potentials (V vs Fc/Fc$^+$) of C_{60} and dumbbells **10_{IS}**, **11_{IM}**, **12_{IS}**, **13_{IM}**. [a]

Compound	E_{red}^1 [V][b]	E_{red}^2 [V][b]	E_{red}^3 [V][b]	E_{red}^4 [V][b]
C_{60}	−1.14	−1.51	−1.98	−2.49
10_{IS}	−1.14	−1.45	−1.91	−2.30
11_{IM}	−1.14	−1.45	−1.91	−2.29
12_{IS}	−1.17	−1.43	−2.00	−2.32
13_{IM}	−1.14	−1.47	−1.94	−2.36

[a] Experimental conditions: V vs ferrocene/ferrocenium (Fc/Fc$^+$); the reference electrode is Ag/AgCl; the working electrode is a glassy carbon electrode (GCE); 0.1 M nBu$_4$NPF$_6$; scan rate: 50 mVs^{-1}; measured in *o*-DCB/dimethylformamide (100 : 1 v/v) at room temperature. [b] Measured by CV.

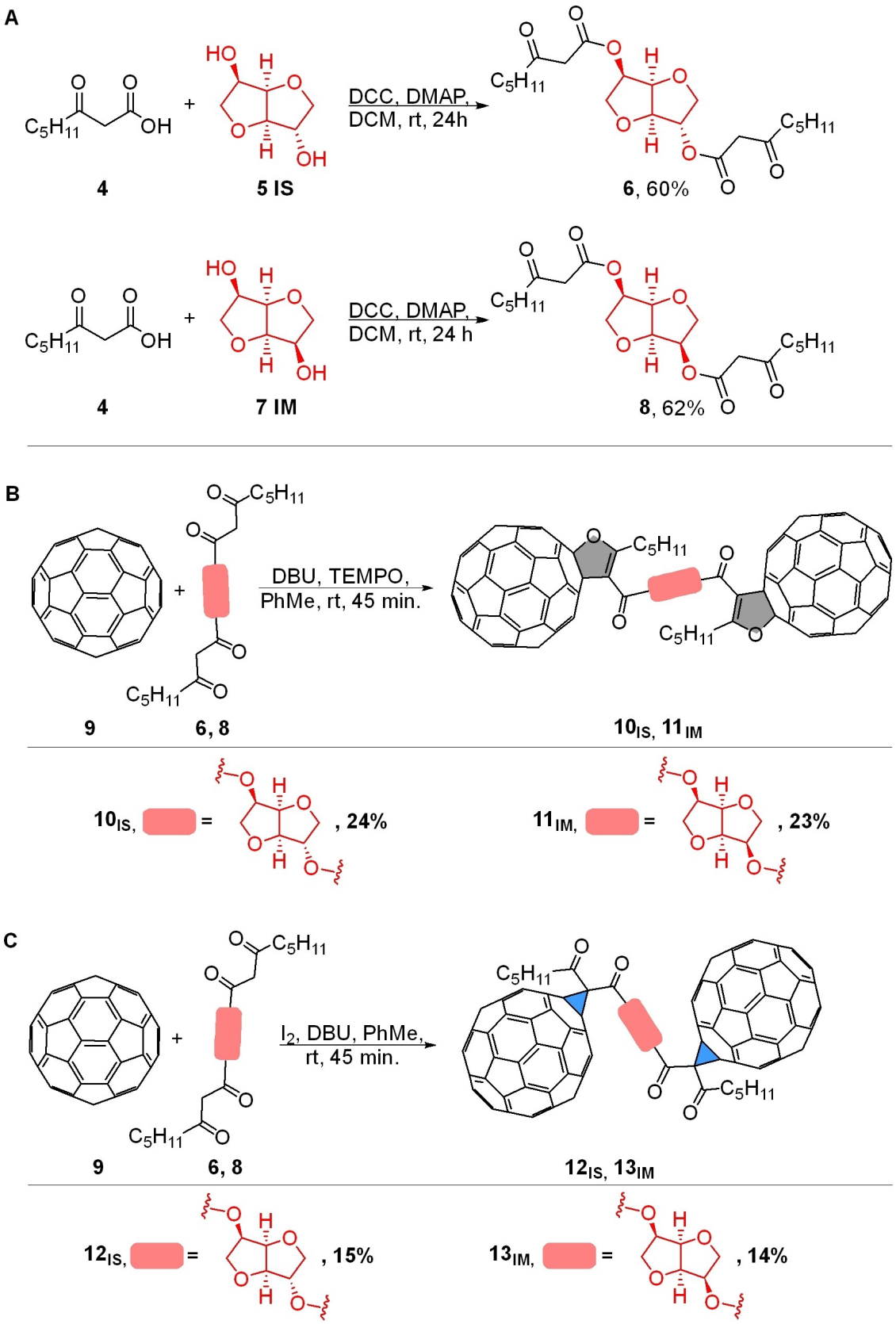

Scheme 1. A Synthesis of the sugar linkers, **B/C** Synthetic pathway for obtaining fullerene dumbbell-like molecule bridged cyclopropane (marked in blue)- and furan-based structures (marked in grey).

to C_{60}. In general, when the C_{2v} symmetry of C_{60} is broken it is harder for the derivative to accept the electron. However, in this case, both types of dumbbells **10_{IS}**, **11_{IM}** and **12_{IS}**, **13_{IM}** showed the same or slightly more negative value for the first reduction, consistent with the established rule.[1] Furthermore, both types of fullerene derivatives show essentially the same CV behaviour.

All four derivatives have also demonstrated stability against oxidation (see Supporting Information, CV). While no significant differences in the electrochemical behavior of the four dumbbell derivatives were observed, varying thermal stabilities were observed depending on the linker used to connect the fullerene moieties. Thermogravimetric analysis (TGA) of the four dumbbell molecules revealed that **11_{IM}** and **13_{IM}** could withstand temperatures up to 200 °C, while **10_{IS}** and **12_{IS}** could withstand temperatures up to 400 °C under inert conditions (see Figure S59). Interestingly, the synthetic strategy (Bingel-Hirsch reaction versus [3+2] cycloaddition of bis-β-keto esters) appears to have a negligible influence on thermal stability but does have an important effect on total weight loss. On the other hand, the sugar moiety clearly determines the thermal stability, with the isosorbide derivatives **10_{IS}** and **12_{IS}** being the most stable.

Since C_{60} fullerene derivatives form very stable complexes with [10]CPPs, the influence of the bridging unit of the four dumbbell-shaped molecules on complex formation with [10]CPP was investigated. For this purpose, ITC was performed in *o*-DCB, because an advantage of this technique is the possibility to perform the titrations in both directions.[18a] On the one hand, the dumbbell molecules can be added to the [10]CPP (dumbbell→[10]CPP), on the other hand, the titration can be performed in reverse, so that the nanohoop is injected into the fullerene derivative ([10]CPP→dumbbell). By analyzing the titrations from both directions using the independent binding site model, the stoichiometry (n) of the complexation process became evident. Subsequently, a global analysis employing appropriate stoichiometric binding models was conducted to obtain the overall binding constants and thermodynamic parameters.[18a] Given that the dumbbell-shaped molecules possess two binding sites, it is anticipated that, in addition to a 1:1 complex [10]CPP⊃dumbbell, a 2:1 complex ([10]CPP)$_2$⊃dumbbell could also be formed. This implies that a stoichiometry of n = 0.5 is expected for the first titration (dumbbell→[10]CPP), while a stoichiometry of n = 2 is anticipated for the reverse titration ([10]CPP→dumbbell).

When comparing the results of the complexation of **10_{IS}**, **11_{IM}**, **12_{IS}** and **13_{IM}** with [10]CPP, it becomes evident that the furan-fused fullerenes **10_{IS}** and **11_{IM}** behave as described above. For **10_{IS}**, the values of n are 0.475 (for dumbbell→[10]CPP) and 1.83 ([10]CPP→dumbbell), as shown in Figures S42 and S43, respectively. Similarly, for **11_{IM}**, the n values are 0.487 (for dumbbell→[10]CPP) and 2.32 ([10]CPP→dumbbell), as seen in Supporting Information Figure S44 and S45. This results clearly indicate the formation of the 2:1 complex ([10]CPP)$_2$⊃**10_{IS}** or ([10]CPP)$_2$⊃**11_{IM}** consisting of two [10]CPP rings and one dumbbell molecule, in addition to the 1:1 complexes. Consequently, a binding model of 1:2 (for dumbbell→[10]CPP) along with 2:1 (for [10]CPP→dumbbell) can be employed for the global analysis of the titrations in both directions, as depicted in Figures S46 and S47. This analysis yields final binding constants and thermodynamic parameters, summarized in Table 2.

For **10_{IS}** and **11_{IM}**, the obtained binding constants range between $7.83 \cdot 104\ M^{-1}$ and $1.28 \cdot 106\ M^{-1}$, aligning well with the binding affinities of previously studied dumbbell molecules[18a] and other malonyl ester-substituted fullerene monoadducts.[22] In the case of **10_{IS}**, the binding constants and the entropic contributions are slightly higher compared to **11_{IM}**, potentially due to the geometry of the molecule. Semi-empirical (PM6) calculations suggest that there is somewhat more space for the binding of two [10]CPPs with **10_{IS}** than is the case of **11_{IM}** (see Figure S56). The species distribution of the titrations with **10_{IS}** and **11_{IM}** reveals that the 1:1 complex is predominantly present during the titrations where there is an excess of dumbbell molecule at the end (dumbbell→[10]CPP). Hence, it is not surprising that in the inverse titration ([10]CPP→dumbbell), the corresponding 2:1 complexes ([10]CPP)$_2$⊃**10_{IS}** or([10]CPP)$_2$ ⊃**11_{IM}** are predominant, as the binding sites can be completely saturated with [10]CPP. However, the behavior of the methanofullerenes **12_{IS}** and **13_{IM}** is different. The analysis using the independent sites model from both directions does not exhibit clear 2:1 stoichiometries. Instead of the anticipated value of n = 0.5, the stoichiometries for the titration of dumbbell→[10]CPP are n = 0.625 for **12_{IS}** (see Figure S48) and n = 0.704 for **13_{IM}** (see Figure S49). Similarly, for the reverse

Table 2. Results of the global analysis with a 1:2 and 2:1 binding model of the ITC titrations from both directions giving final binding affinities and thermodynamic parameters for the complexation of the four different dumbbell molecules with [10]CPP.

Dumbbell molecule	K_a [M^{-1}]	ΔH [kcal mol^{-1}]	ΔG [kcal mol^{-1}]	ΔS [cal mol^{-1} K^{-1}]
10_{IS}	$K_1 = (1.28 \pm 0.08) \cdot 10^6$	$\Delta H_1 = -5.28 \pm 0.07$	$\Delta G_1 = -8.33$	$\Delta S_1 = 10.2$
	$K_2 = (1.26 \pm 0.11) \cdot 10^5$	$\Delta H_2 = -4.92 \pm 0.19$	$\Delta G_2 = -6.95$	$\Delta S_2 = 6.83$
11_{IM}	$K_1 = (1.49 \pm 0.11) \cdot 10^5$	$\Delta H_1 = -5.95 \pm 0.03$	$\Delta G_1 = -7.06$	$\Delta S_1 = 3.71$
	$K_2 = (7.83 \pm 0.60) \cdot 10^4$	$\Delta H_2 = -5.46 \pm 0.03$	$\Delta G_2 = -6.67$	$\Delta S_2 = 4.07$
12_{IS}	$K_1 = (6.86 \pm 0.24) \cdot 10^5$	$\Delta H_1 = -8.21 \pm 0.12$	$\Delta G_1 = -7.96$	$\Delta S_1 = -8.60$ [a]
	$K_2 = (1.58 \pm 0.10) \cdot 10^4$	$\Delta H_2 = -9.78 \pm 0.17$	$\Delta G_2 = -5.72$	$\Delta S_2 = -13.6$ [a]
13_{IM}	$K_1 = (3.47 \pm 0.24) \cdot 10^5$	$\Delta H_1 = -6.63 \pm 0.11$	$\Delta G_1 = -7.55$	$\Delta S_1 = 3.11$
	$K_2 = (1.71 \pm 0.23) \cdot 10^4$	$\Delta H_2 = -4.12 \pm 0.29$	$\Delta G_2 = -5.77$	$\Delta S_2 = 5.54$

[a] Due to the bigger deviation from the applied fitting model to the experimental values for **12_{IS}** (see Supporting Information, Figure S52), the error in the determination of enthalpy and entropy is quite large. For this reason, other binding models are proposed (see below). However, despite the different sign, the absolute values of the entropic term (cal mol^{-1}) are almost negligible compared to the enthalpic contribution (kcal mol^{-1}).

experiment ([10]CPP→dumbbell), the values deviate significantly from the expected value of 2, with n = 1.40 for $\mathbf{12}_{IS}$ (see Figure S50) and n = 1.21 for $\mathbf{13}_{IM}$ (see Figure S51). Figure 1 illustrates the representative thermograms of the titrations with $\mathbf{13}_{IM}$ in both directions, along with the corresponding fitting curves and the resulting species distributions from the global analysis.

Nevertheless, the global analysis for $\mathbf{12}_{IS}$ (see Figure S52) and $\mathbf{13}_{IM}$ (see Figure S53) yields binding constants that are of a similar order of magnitude compared to the values of $\mathbf{11}_{IM}$ (see Table 2).

However, despite the reasonably acceptable results obtained from the global analysis, it is evident that other processes contribute to the altered stoichiometries observed in the titrations of [10]CPP with $\mathbf{12}_{IS}$ or $\mathbf{13}_{IM}$. Since the stoichiometries do not clearly correspond to other defined binding models (e.g., 1:1), fitting these models resulted in worse outcomes compared to the 1:2 and 2:1 binding models shown in Figure 1. In order to gain further insights into the actual binding behavior of the methanofullerenes with [10]CPP, NMR titrations of $\mathbf{13}_{IM}$ and [10]CPP were performed in both directions (Figure 2a and Figures S54–S55), as this molecule exhibited the most significant deviations from the expected values. Although NMR titrations allow for higher ratios between the dumbbell molecule and [10]CPP compared to ITC measurements, the change in chemical shift still cannot be unambiguously fit with simple binding models. However, the additional broadening of the peaks during the titrations indicates the occurrence of coalescence phenomena. To investigate this further, NMR spectra at variable temperatures were recorded (see Figure 2b), in order to draw conclusions about the complex composition.

The first temperature series was recorded at a ratio of [10]CPP:$\mathbf{13}_{IM}$ 1:0.5 (see Figure 2b). A clear splitting of the [10]CPP proton signal can be observed starting at 0 °C. It was expected that at this ratio, the [10]CPP protons would split into two approximately symmetric signals, since complexation causes the protons pointing toward the bridging unit to have a different chemical shift than the protons pointing in the other direction.[16] However, the ratio of these signal changes with increasing amounts of $\mathbf{13}_{IM}$ (see Figure 2c). One possible explanation for this is that, in addition to the 1:1 [10]CPP⊃$\mathbf{13}_{IM}$ and 2:1 ([10]CPP)$_2$⊃$\mathbf{13}_{IM}$ complexes, the 1:2 [10]CPP⊃($\mathbf{13}_{IM}$)$_2$ complex or a linear oligomer might be also formed, as indicated by the schematic illustration in Figure 2c. The third distinct signal in Figure 2c at about 7.47 ppm could be assigned to the free [10]CPP. However, this signal disappears with increasing amount of $\mathbf{13}_{IM}$ (see Figure 2c). The different splitting and signal ratios of the investigated mixtures indicates how different the composition of the complexes must be, which explains why neither the ITC data nor the NMR data could be fitted with simple binding models, as multiple complexes with different stoichiometries are formed during the titrations.

In addition, geometry optimizations were performed using the BLYP function (improved with the Grimme correction for dispersion (D3)) and the 6–31G** basis set) for the isomannide-bridged derivatives $\mathbf{11}_{IM}$ and $\mathbf{13}_{IM}$. DFT calculations revealed that, in the case of $\mathbf{13}_{IM}$, the two C_{60} spheres are in close proximity to each other, preventing the free approach of [10]CPP. This is not the case for the rigid $\mathbf{11}_{IM}$, where the fullerene units have a maximum distance (see Supporting Information, Figures S57 and S58).

The formation of linear oligomers holds great promise for their incorporation in the active layer of bulk-heterojunction cells. This approach could offer the control over morphology and phase separation, improve interconnectivity, as well as increase the donor-acceptor interface. These factors collectively contribute to efficient charge generation, transport, and collection, resulting in enhanced device performance in organic

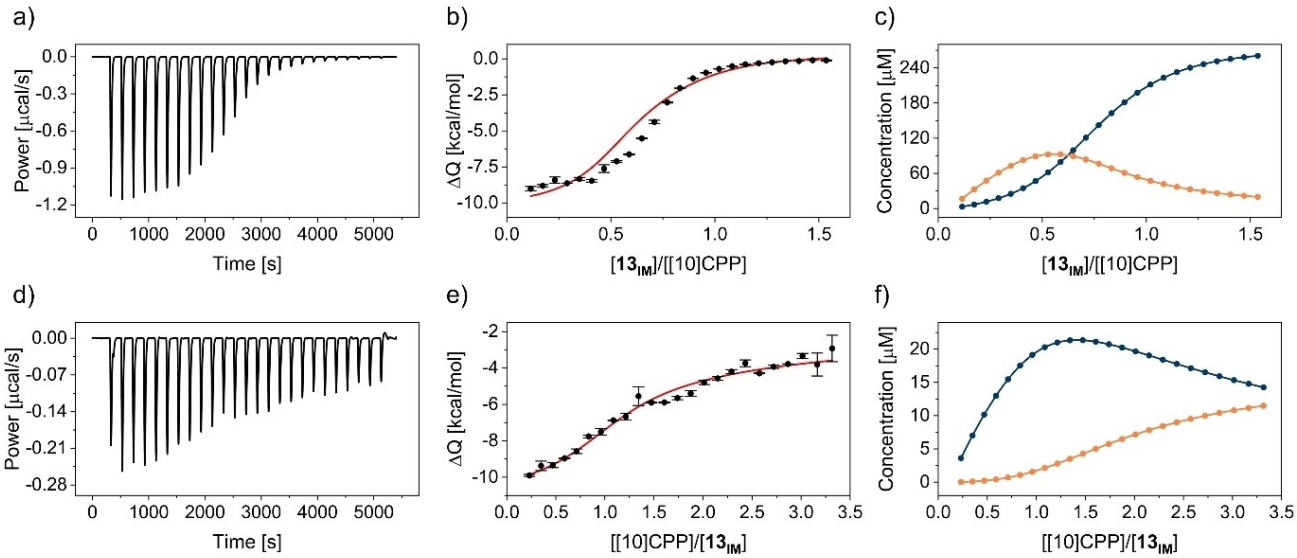

Figure 1. Exemplary ITC data of the global analysis of the titrations in *o*-DCB in the two different directions: $\mathbf{13}_{IM}$→ [10]CPP (a–c) and [10]CPP →$\mathbf{13}_{IM}$ (d–f). Experimental thermograms (a, d), fitting curves (red) using a 1:2 (b) and 2:1 (e) binding model from AFFINImeter software and species distribution of [10]CPP ⊃$\mathbf{13}_{IM}$ (blue) and ([10]CPP)$_2$⊃$\mathbf{13}_{IM}$ (orange) (c,f).

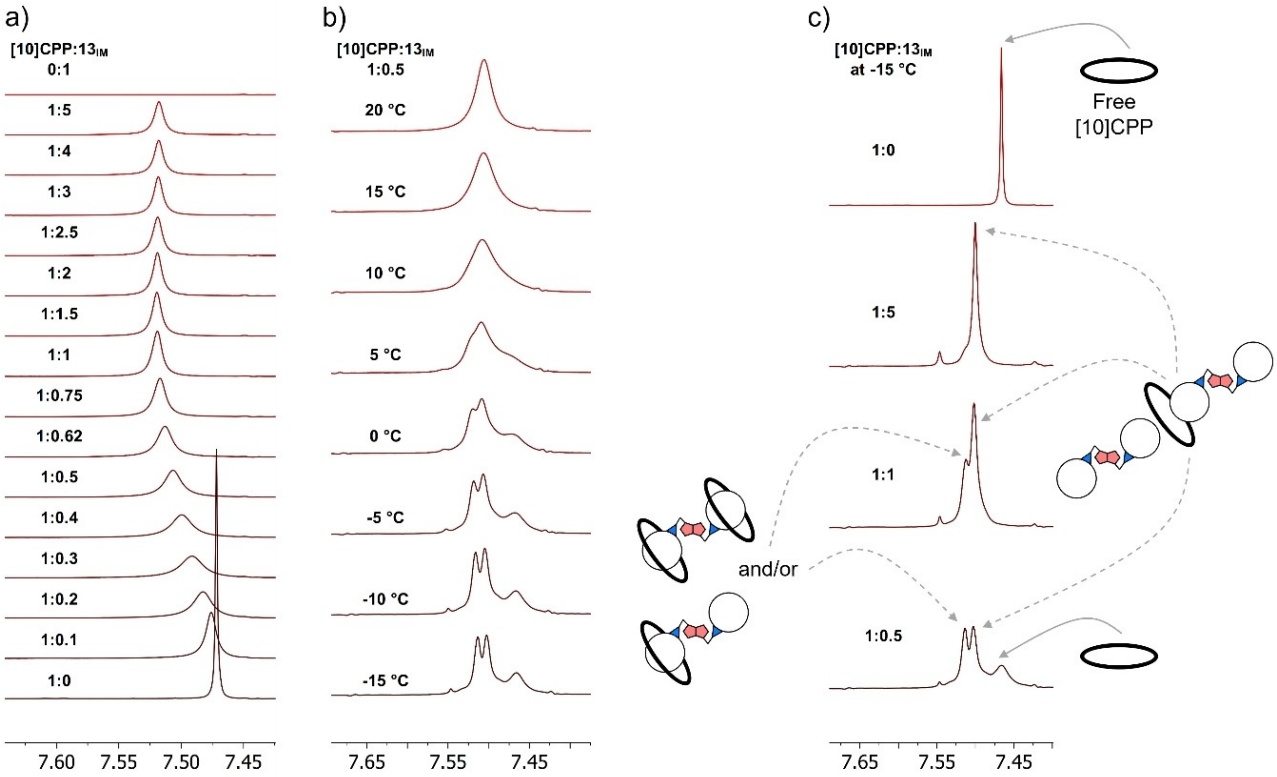

Figure 2. a) Section of the ^{1}H NMR (600 MHz) spectra of the titration $\mathbf{13}_{IM}$→[10]CPP in $C_6D_4Cl_2$ showing the [10]CPP signal. b) Temperature-dependent ^{1}H NMR (600 MHz) spectra of the [10]CPP: $\mathbf{13}_{IM}$ mixture with a ratio of 1:0.5. c) Comparison of the ^{1}H NMR (600 MHz) spectra showing the different splitting of the [10]CPP signal of various mixtures at −15 °C with the free [10]CPP signal.

photovoltaics.[5b] Moreover, the thermal and oxidative stability of the dumbbells, as evidenced before, further supports their potential for application in such devices.

Conclusions

A series of unprecedented sugar-bridged fullerene dumbbells was synthesized and thoroughly characterized. Methano- and furan-fused C_{60} derivatives exhibited high solubility in common organic solvents and demonstrated the capacity to accept up to eight electrons in reduction processes. Furthermore, these molecules displayed interaction with [10]CPP, an electron-donating nanoring, leading to the formation of pseudorotaxanes. Notably, the methano-dumbbell molecules $\mathbf{12}_{IS}$ and $\mathbf{13}_{IM}$ showed different binding behaviour with [10]CPP compared to the furan-fused molecules $\mathbf{10}_{IS}$ and $\mathbf{11}_{IM}$, where conventional 2:1 complexes were formed. The difference in stereochemistry between the isomannide and isosorbide moieties did not affect the complex formation. However, the presence of a cyclopropane linkage on the sphere introduced higher degrees of freedom, inhibiting the formation of a single bis-pseudorotaxane product. The species distribution in the derivatives $\mathbf{12}_{IS}$ and $\mathbf{13}_{IM}$ is likely due to the proximity of C_{60} units, which hinders cofacial π-π stacking interactions with [10]CPP. Among these supramolecular interactions, the formation of oligomers (polymers) based on C_{60} dumbbell molecules holds particular significance, as these systems are promising for sustainable solar energy conversion.

Experimental Section

Preparation of dumbbell-like furan-fused fullerenes ($\mathbf{10}_{IS}$, $\mathbf{11}_{IM}$): DBU (39 μL, 0.26 mmol, 20 equiv.) was added to the solution of C_{60} **9** (30 mg, 42 μmol, 3 equiv.), bis β-keto ester-isohexide derivate **6** or **8** (5.5 mg, 13 μmol, 1 equiv.) and TEMPO (4.1 mg, 26 μmol, 2 equiv.) in toluene (30 mL). The reaction mixture was stirred for 45 min at room temperature, under an argon atmosphere. Once the reaction was completed, the reaction mixture was filtrated through a silica gel pad and washed with toluene. The solvent was then removed under reduced pressure, and the residue was chromatographed on a silica gel column with petrol ether as eluent, to recover unreacted C_{60}. Further elution with toluene/petroleum ether (7:3 *v/v*) gave pure product $\mathbf{10}_{IS}$ and $\mathbf{11}_{IM}$, respectively.

Compound $\mathbf{10}_{IS}$: 5.8 mg, 24%, brown solid; ^{1}H NMR (400 MHz, $CDCl_3/CS_2$): δ 5.42 (d, J=2.9 Hz, **C2**-1H), 5.30 (dd, J_1=11.9 Hz, J_2=6.2 Hz, **C5**-1H), 4.63 (t, J=4.7 Hz, **C4**-1H), 4.54 (d, J=4.2 Hz, **C3**-1H), 4.03 (dd, J_1=9.3 Hz, J_2=6.7 Hz, **C6**-1H), 3.95 (d, J=10.7 Hz, **C1**-1H), 3.82 (dd, J_1=10.6 Hz, J_2=3.4 Hz, **C1**-1H), 3.67 (dd, J_1=9.3 Hz, J_2=6.6 Hz, **C6**-1H), 3.36–3.26 (m, 4H), 2.06 (quin, J=7.5 Hz, 4H), 1.69–1.62 (m, 4H), 1.56–1.51 (m, 4H), 1.05–1.01 (m, 6H) ppm; ^{13}C NMR (100 MHz, $CDCl_3/CS_2$): δ 175.1, 174.8, 164.0, 163.5, 148.5, 148.4, 148.3, 148.2, 147.5, 147.1, 146.6, 146.4, 146.3, 146.21, 146.15, 145.8, 145.6, 145.4, 145.2, 144.9, 144.7, 144.4, 142.94, 142.88, 142.65,

142.61, 142.5, 141.8, 141.6, 140.0, 139.50, 139.47, 139.4, 137.6, 135.5, 104.3, 104.2, 103.3 (sp^3-C of C_{60}), 103.2 (sp^3-C of C_{60}), 86.0, 81.0, 78.4, 74.5, 73.4, 72.1 (sp^3-C of C_{60}), 72.0 (sp^3-C of C_{60}), 70.0, 31.9, 29.2, 27.0, 22.7, 14.3 ppm; IR (ATR): ν 2950, 2924, 2865, 1705, 1627, 1427, 1307, 1172, 1124, 1081, 974, 946, 796, 526 cm^{-1}; UV-vis ($CHCl_3$): λ 429, 457, 483, 687 nm (ε = 7296, 5874, 4848, 839 $dm^3\ mol^{-1}\ cm^{-1}$); Positive HRMS (MALDI): m/z): calcd for $[M+H]^{+\bullet}$ $[C_{142}H_{30}O_8+H]^+$:1864.2047; found, 1864.758.

Compound 11_{IM}: 5.5 mg, 23%, brown solid; ^{1}H NMR (500 MHz, $CDCl_3/CS_2$): δ 5.33–5.27 (m, **C2**-1H, **C5**-1), 4.83–4.78 (m, **C4**-1H, **C3**-1), 4.04 (dd, J_1 = 8.8 Hz, J_2 = 7.2 Hz, **C6**-1H, **C1**-1H), 3.46 (t, J = 8.5 Hz, **C1**-1H, **C6**-1H), 3.38–3.22 (m, 4H), 2.05 (quin, J = 7.6 Hz, 4H), 1.67–1.61 (m, 4H), 1.56–1.51 (m, 4H), 1.02 (t, J = 7.3 Hz, 6H) ppm; ^{13}C NMR (125 MHz, $CDCl_3/CS_2$): δ 175.0, 163.9, 148.5, 148.4, 148.2, 147.6, 147.5, 147.2, 146.6, 146.4, 146.2, 146.1, 145.83, 145.80, 145.6, 145.5, 145.4, 145.2, 144.93, 144.90, 144.7, 144.6, 144.5, 144.4, 143.0, 142.93, 142.87, 142.71, 142.65, 142.56, 142.49, 142.47, 142.44, 141.8, 141.7, 141.6, 140.1, 139.4, 139.2, 137.7, 137.6, 135.5, 104.2, 103.2 (sp^3-C of C_{60}), 80.5, 74.4, 73.4, 72.0 (sp^3-C of C_{60}), 69.9, 31.9, 29.2, 27.1, 22.7, 14.3 ppm; IR (ATR): ν 2949, 2920, 2865, 1704, 1626, 1426, 1323, 1173, 1125, 1082, 974, 946, 795, 526 cm^{-1}; UV-Vis ($CHCl_3$): λ 429, 457, 483, 687 nm (ε = 8756, 6642, 5224, 821 $dm^3\ mol^{-1}\ cm^{-1}$). Positive HRMS (APCI): calcd for $[M+H]^{+\bullet}$ $[C_{142}H_{30}O_8+H]^{+\bullet}$: 1864.2047; found, 1864.1929.

Preparation of dumbbell-like metanofullerenes (12_{IS}, 13_{IM}): DBU (6.0 μL, 40 μmol, 3 equiv.) was added to the solution of C_{60} **9** (30 mg, 42 μmol, 3 equiv.), bis β-keto ester-isohexide derivate **6** or **8** (5.5 mg, 13 μmol, 1 equiv.) and iodine (10.1 mg, 40 μmol, 3 equiv.) in toluene (30 mL). The reaction mixture was stirred for 45 min at room temperature, under an argon atmosphere. After the reaction was completed, the reaction mixture was filtrated through a silica gel pad and washed with toluene, the solvent was removed under reduced pressure. The obtained crude product was chromatographed on a silica gel column with petrol ether as eluent, to recover unreacted C_{60}. Further elution with toluene/petroleum ether (7 : 3 *v/v*) gave pure product 12_{IS}, and 13_{IM}, respectively.

Compound 12_{IS}: 3.6 mg, 15%, brown solid; ^{1}H NMR (400 MHz, $CDCl_3$): δ 5.67 (s, **C2**-1H), 5.60–5.55 (m, **C5**-1H), 5.16 (t, J = 5.3 Hz, **C4**-1H), 4.79 (d, J = 4.9 Hz, **C3**-1H), 4.24–4.09 (m, **C6**-2H, **C1**-2H), 3.38–3.27 (m, 2H), 3.23 (t, J = 7.1 Hz, 2H), 1.97–1.83 (m, 4H), 1.48–1.36 (m, 8H), 0.99–0.91 (m, 6H) ppm; ^{13}C NMR (100 MHz, $CDCl_3$): δ 196.1, 196.0, 163.7, 163.4, 145.5, 145.42, 145.40, 145.37, 145.05, 145.02, 144.90, 144.88, 144.85, 144.83, 144.77, 144.02, 143.99, 143.34, 143.28, 143.22, 143.19, 143.1, 142.4, 142.1, 142.0, 141.9, 141.2, 139.4, 139.14, 139.06, 138.4, 138.2, 86.2, 81.3, 80.6, 76.6, 73.3, 73.0 (sp^3-C of C_{60}), 72.4 (sp^3-C of C_{60}), 72.24 (sp^3-C of C_{60}), 72.19 (sp^3-C of C_{60}), 71.23, 59.2, 58.8, 41.5, 41.2, 31.5, 31.4, 23.8, 23.7, 22.7 (**2 C**), 14.2, 14.1 ppm; IR (ATR): ν 2949, 2921, 2853, 1723, 1225, 1178, 1094, 754, 525 cm^{-1}; UV-Vis ($CHCl_3$): λ 426, 492, 690 nm (ε = 7052, 4832, 205 $dm^3\ mol^{-1}\ cm^{-1}$); Positive HRMS (MALDI): calcd for $[M+H]^{+\bullet}$ $[C_{142}H_{30}O_8+H]^+$:1864.2047; found, 1864.822.

Compound 13_{IM}: 3.4 mg, 14%, brown solid; ^{1}H NMR (500 MHz, $CDCl_3$): δ 5.51–5.44 (m, **C5**-1H, **C2**-1H), 5.08 (d, J = 4.3 Hz, **C4**-1H, C3-1H), 4.26 (dd, J_1 = 9.6 Hz, J_2 = 6.6 Hz, **C6**-1H, **C1**-1H), 4.09 (dd, J_1 = 9.6 Hz, J_2 = 7.0 Hz, **C6**-1H, **C1**-1H), 3.41–3.26 (m, 4H), 1.98–1.86 (m, 4H), 1.52–1.38 (m, 8H), 0.95 (t, J = 7.0 Hz, 6H) ppm; ^{13}C NMR (125 MHz, $CDCl_3$): δ 196.0, 163.8, 145.8, 145.43, 145.38, 145.3, 145.2, 145.1, 145.0, 144.9, 144.84, 144.79, 144.7, 144.0, 143.34, 143.28, 143.23, 143.19, 143.16, 142.40, 142.37, 142.1, 142.02, 142.00, 141.25, 141.19, 139.24, 139.1, 138.4, 138.3, 80.6, 76.4, 72.42 (sp^3-C of C_{60}), 72.37 (sp^3-C of C_{60}), 70.6, 59.2, 41.2, 31.5, 23.6, 22.7, 14.2 ppm; IR (ATR): ν 2952, 2926, 2861, 1725, 1228, 1182, 905, 730, 526 cm^{-1}; UV-Vis ($CHCl_3$): λ 426, 492, 690 nm (ε = 8392, 4918, 513 $dm^3\ mol^{-1}\ cm^{-1}$). Positive HRMS (APCI): calcd for $[M+H]^{+\bullet}$ $[C_{142}H_{30}O_8+H]^{+\bullet}$: 1864.2047; found, 1864.1958.

Supporting Information

Additional references cited within the Supporting Information.[23]

The Supporting Information section includes all of the experimental protocols, NMR, UV/Vis, and FTIR spectra, as well as information on cyclic voltammetry and isothermal titration calorimetry measurements. Additionally, it provides details on the NMR titration experiments and includes DFT calculations and thermal stability studies.

Acknowledgements

The authors would like to thank the Ministry of Education, Science and Technological Development of Republic of Serbia (contract number: 451-03-9/2021-14/200168). We thank the Deutsche Forschungsgemeinschaft (DFG) for the financial support of this work through the SFB 953 (project number 182849149) "Synthetic Carbon Allotropes" projects A1 and A9. A. M. thanks Alexander von Humboldt (AvH) for equipment grant (Autolab) and for sponsorship for Renewed research stay. We thank Dr. Dušan Veljković for carrying out the DFT calculations and for fruitful discussions regarding the geometry of the molecules. We also thank Florian Steiger and Vincent Wedler for their help with the TGA measurements.

Conflict of Interests

The authors declare no conflict of interest.

Data Availability Statement

The data that support the findings of this study are available from the corresponding author upon reasonable request.

Keywords: dumbbells · fullerenes · isomannides · isosorbides · pseudorotaxanes

[1] M. H. BinSabt, H. M. Al-Matar, A. L. Balch, M. A. Shalaby, *ACS Omega* **2021**, *6*, 20321–20330.
[2] a) Y. N. Biglova, A. G. Mustafin, *RSC Adv.* **2019**, *9*, 22428–22498; b) Y. N. Biglova, *Beilstein J. Org. Chem.* **2021**, *17*, 630–670.
[3] M. Maggini, G. Scorrano, M. Prato, *J. Am. Chem. Soc.* **1993**, *115*, 9798–9799.
[4] a) Y. Rubin, S. Khan, D. I. Freedberg, C. Yeretzian, *J. Am. Chem. Soc.* **1993**, *115*, 344–345; b) P. Hudhomme, *C. R. Chim.* **2006**, *9*, 881–891.
[5] a) A. B. Atar, *Synlett* **2019**, *30*, 1462–1468; b) B. C. Schroeder, Z. Li, M. A. Brady, G. C. Faria, R. S. Ashraf, C. J. Takacs, J. S. Cowart, D. T. Duong, K. H. Chiu, C.-H. Tan, J. T. Cabral, A. Salleo, M. L. Chabinyc, J. R. Durrant, I. McCulloch, *Angew. Chem. Int. Ed.* **2014**, *53*, 12870–12875.
[6] a) T. W. Chamberlain, E. S. Davies, A. N. Khlobystov, N. R. Champness, *Chem. Eur. J.* **2011**, *17*, 3759–3767; b) M. E. Pérez-Ojeda, N. Zink-Lorre, S.

Pla, A. Zink, Á. Sastre-Santos, F. Fernández-Lázaro, A. Hirsch, *Dyes Pigm.* **2022**, *199*, 110044.
[7] A. Mitrović, J. Stevanović, M. Milčić, A. Žekić, D. Stanković, S. Chen, J. D. Badjić, D. Milić, V. Maslak, *RSC Adv.* **2015**, *5*, 88241–88248.
[8] A. S. Konev, A. F. Khlebnikov, H. Frauendorf, *J. Org. Chem.* **2011**, *76*, 6218–6229.
[9] A. La Rosa, K. Gillemot, E. Leary, C. Evangeli, M. T. González, S. Filippone, G. Rubio-Bollinger, N. Agraït, C. J. Lambert, N. Martín, *J. Org. Chem.* **2014**, *79*, 4871–4877.
[10] T. Wei, M. E. Pérez-Ojeda, A. Hirsch, *Chem. Commun.* **2017**, *53*, 7886–7889.
[11] a) K. Calderon Cerquera, A. Parra, D. Madrid-Úsuga, A. Cabrera-Espinoza, C. A. Melo-Luna, J. H. Reina, B. Insuasty, A. Ortiz, *Dyes Pigm.* **2021**, *184*, 108752; b) L. Huang, X. Yu, W. Wu, J. Zhao, *Org. Lett.* **2012**, *14*, 2594–2597.
[12] a) J.-F. Nierengarten, J.-F. Eckert, D. Felder, J.-F. Nicoud, N. Armaroli, G. Marconi, V. Vicinelli, C. Boudon, J.-P. Gisselbrecht, M. Gross, G. Hadziioannou, V. Krasnikov, L. Ouali, L. Echegoyen, S.-G. Liu, *Carbon* **2000**, *38*, 1587–1598; b) H. Suguru, I. Hiroshi, K. Takahiro, S. Yoshiteru, *Chem. Lett.* **1998**, *27*, 605–606.
[13] a) E. Nuin, W. Bauer, A. Hirsch, *Eur. J. Org. Chem.* **2017**, *2017*, 790–798; b) N. Armaroli, F. Diederich, C. O. Dietrich-Buchecker, L. Flamigni, G. Marconi, J.-F. Nierengarten, J.-P. Sauvage, *Chem. Eur. J.* **1998**, *4*, 406–416; c) M. D. Meijer, G. P. M. van Klink, G. van Koten, *Coord. Chem. Rev.* **2002**, *230*, 141–163.
[14] C.-H. Andersson, L. Nyholm, H. Grennberg, *Dalton Trans.* **2012**, *41*, 2374–2381.
[15] T. Iwamoto, Y. Watanabe, T. Sadahiro, T. Haino, S. Yamago, *Angew. Chem. Int. Ed.* **2011**, *50*, 8342–8344.
[16] Y. Xu, R. Kaur, B. Wang, M. B. Minameyer, S. Gsänger, B. Meyer, T. Drewello, D. M. Guldi, M. von Delius, *J. Am. Chem. Soc.* **2018**, *140*, 13413–13420.
[17] Y. Xu, B. Wang, R. Kaur, M. B. Minameyer, M. Bothe, T. Drewello, D. M. Guldi, M. von Delius, *Angew. Chem. Int. Ed.* **2018**, *57*, 11549–11553.
[18] a) I. Solymosi, J. Sabin, H. Maid, L. Friedrich, E. Nuin, M. E. Pérez-Ojeda, A. Hirsch, *Org. Mater.* **2022**, *4*, 73–85; b) M. Freiberger, M. B. Minameyer, I. Solymosi, S. Frühwald, M. Krug, Y. Xu, A. Hirsch, T. Clark, D. M. Guldi, M. von Delius, K. Amsharov, A. Görling, M. E. Pérez-Ojeda, T. Drewello, *Chem. - Eur. J.* **2023**, *29n/a*, e202203734; c) M. Freiberger, I. Solymosi, E. M. Freiberger, A. Hirsch, M. E. Pérez-Ojeda, T. Drewello, *Nanoscale* **2023**, *15*, 5665–5670.
[19] A. C. Cope, T. Y. Shen, *J. Am. Chem. Soc.* **1956**, *78*, 3177–3182.
[20] J. Jakšić, A. Mitrović, Z. Tokić Vujošević, M. Milčić, V. Maslak, *RSC Adv.* **2021**, *11*, 29426–29432.
[21] M. T. Beck, G. Mándi, *Fullerene Sci. Technol.* **1997**, *5*, 291–310.
[22] J. Volkmann, D. Kohrs, H. A. Wegner, *Chem. - Eur. J.* <**2023**, *29 n/a*, e202300268.
[23] a) J. T. Hodgkinson, W. R. J. D. Galloway, M. Casoli, H. Keane, X. Su, G. P. C. Salmond, M. Welch, D. R. Spring, *Tetrahedron Lett.* **2011**, *52*, 3291–3294; b) J. Radivojevic, S. Skaro, L. Senerovic, B. Vasiljevic, M. Guzik, S. T. Kenny, V. Maslak, J. Nikodinovic-Runic, K. E. O'Connor, *Appl. Microbiol. Biotechnol.* **2016**, *100*, 161–172; c) G. W. T. M. J. Frisch, H. B. Schlegel, G. E. Scuseria, M. A. Robb, J. R. Cheeseman, G. Scalmani, V. Barone, G. A. Petersson, H. Nakatsuji, X. Li, M. Caricato, A. Marenich, J. Bloino, B. G. Janesko, R. Gomperts, B. Mennucci, H. P. Hratchian, J. V. Ortiz, A. F. Izmaylov, J. L. Sonnenberg, D. Williams-Young, F. Ding, F. Lipparini, F. Egidi, J. Goings, B. Peng, A. Petrone, T. Henderson, D. Ranasinghe, V. G. Zakrzewski, J. Gao, N. Rega, G. Zheng, W. Liang, M. Hada, M. Ehara, K. Toyota, R. Fukuda, J. Hasegawa, M. Ishida, T. Nakajima, Y. Honda, O. Kitao, H. Nakai, T. Vreven, K. Throssell, J. A. Montgomery, Jr., J. E. Peralta, F. Ogliaro, M. Bearpark, J. J. Heyd, E. Brothers, K. N. Kudin, V. N. Staroverov, T. Keith, R. Kobayashi, J. Normand, K. Raghavachari, A. Rendell, J. C. Burant, S. S. Iyengar, J. Tomasi, M. Cossi, J. M. Millam, M. Klene, C. Adamo, R. Cammi, J. W. Ochterski, R. L. Martin, K. Morokuma, O. Farkas, J. B. Foresman, D. J. Fox, *Gaussian, Inc., Wallingford CT* **2016**; d) A. D. Becke, *Phys. Rev. A* **1988**, *38*, 3098–3100; e) C. Lee, W. Yang, R. G. Parr, *Phys. Rev. B* **1988**, *37*, 785–789; f) M. D. Hanwell, D. E. Curtis, D. C. Lonie, T. Vandermeersch, E. Zurek, G. R. Hutchison, *J. Cheminf.* **2012**, *4*, 17.

Manuscript received: April 3, 2023
Accepted manuscript online: May 18, 2023
Version of record online: ■■, ■■

RESEARCH ARTICLE

Novel sugar-bridged fullerene dumbbells were synthesized and fully characterized. Methano- and furan-fused C_{60} interacted with [10]CPP, an electron-donating nanoring, to form bis-pseudorotaxanes. Interestingly, the methano-dumbbell molecules showed a different binding behaviour as mono-, bis-pseudorotaxanes as well as oligomers (polymers) were detected.

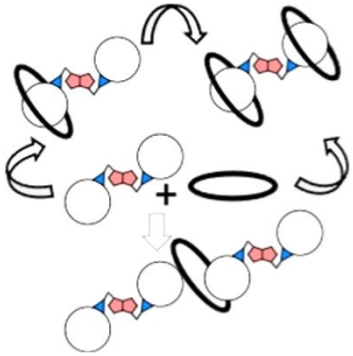

J. Jakšić, I. Solymosi, Prof. Dr. A. Hirsch, Dr. M. E. Pérez-Ojeda, Dr. A. Mitrović*, Dr. V. Maslak**

1 – 9

Sugar-Bridged Fullerene Dumbbells and Their Interaction with the [10]Cycloparaphenylene Nanoring